Acta Cryst. (1994). D**50**, 50–63

Structure of the Recombinant *Paramecium tetraurelia* Calmodulin at 1.68 Å Resolution

BY CHANGILL BAN AND B. RAMAKRISHNAN

Laboratory of Biological Macromolecular Structure, Department of Chemistry, Biochemistry and Biotechnology Center, The Ohio State University, 1060 Camark Road, Columbus, OH 43210, USA

KIT-YIN LING AND CHING KUNG

Laboratory of Molecular Biology, University of Wisconsin-Madison, 1450 Linden Drive, Madison, WI 53706, USA

AND M. SUNDARALINGAM*

Laboratory of Biological Macromolecular Structure, Department of Chemistry, Biochemistry and Biotechnology Center, The Ohio State University, 1060 Camark Road, Columbus, OH 43210, USA

(*Received* 28 *January* 1993; *accepted* 27 *July* 1993)

Abstract

The crystal structure of the recombinant calmodulin from *Paramecium tetraurelia* (rPCaM, M_r = 16 700, 148 residues) has been determined at 1.68 Å resolution. X-ray intensity data were collected at 263 K using a Siemens–Nicolet area detector and Cu $K\alpha$ radiation from a rotating-anode source. A total of 35 936 observations were processed with *XENGEN*1.3 and scaled to yield 16 255 unique reflections with $R_{symm}(I)$ of 4.1%. The crystals are triclinic, with unit-cell dimensions a = 29.89, b = 53.42, c = 25.35 Å, α = 93.67, β = 96.88, γ = 89.24°, space group $P1$, with one molecule in the unit cell. The atomic coordinates of the wild-type *Paramecium* calmodulin (PCaM) studied in our laboratory provided the starting model. Refinement of the structure by *X-PLOR* and refitting it into omit maps yielded an R value of 0.194 for 15 965 reflections greater than $3\sigma(F)$ in the 6.0–1.68 Å resolution range. The final model contained 1165 protein atoms for all of the 148 residues, four Ca^{2+} ions, and 172 water molecules. The dumbbell structure has seven α-helices including a long 7.8 turn central helix connecting the two terminal domains each containing two *EF*-hand (helix–loop–helix motif) calcium-binding sites. The loops within each pair of *EF*-hand motifs in the N- and C-terminal domains are brought into juxtaposition to form a pair of hydrogen-bonded antiparallel β-sheets which are extended at either ends by water bridges. The four calcium-binding *EF*-hands are superposable with r.m.s. deviations of 0.31–0.79 Å. The best agreement is between site 1 and site 3 and the worst agreement is between site 1 and 4. The largest differences are in the ninth and tenth residues of the calcium-binding loops probably because of their involvement in the mini β-sheets. The calcium coordination distances vary between 2.04 and 2.69 Å, average 2.34 Å. The rPCaM and wild-type PCaM have an r.m.s. deviation of 0.36 Å for equivalent C^α atoms. The side chains of Lys13 and Lys115 are more extended in rPCaM compared to the wild type where the post-translational modified di- and tri-methylated lysine residues are more folded. The sequence of PCaM differs from those of mammalian (MCaM) and *Drosophila* calmodulin (DCaM), but the overall structures are very similar, with r.m.s. deviations of 0.44 and 1.68 Å for equivalent C^α atoms, respectively. However, in rPCaM, the first four N-terminal residues stretch out and make intermolecular crystal contacts, in contrast to those in recombinant *Drosophila* calmodulin (rDCaM), they stretch out in the opposite direction and towards the second calcium-binding site (see note below), while in MCaM and wild-type PCaM, the N-terminal residues are not visible. The central helix in rPCaM has all its backbone hydrogen bonds intact with no unusually long separation between the carbonyl and amide groups as found in MCaM and rDCaM.

Introduction

Calmodulin has a variety of physiological functions in eukaryotes (Klee & Vanaman, 1982; Means, Tash

* To whom correspondence should be addressed.

& Chafouleas, 1982). This small acidic protein ($M_r \simeq$ 16 700) mediates the Ca^{2+}-induced intracellular regulation and is activated by the binding of four calcium ions (Tanaka & Hidaka, 1980). It has long been recognized that calcium binding induces significant conformational changes in calmodulin, and these conformational changes enable calmodulin to regulate and activate the target enzymes (Burger, Cox, Comte & Stein, 1984). The structure of the related protein troponin C (Satyshur *et al.*, 1988; Herzberg & James, 1988) had revealed that the calcium-bound C-terminal domain is different from the calcium-free N-terminal domain providing the first atomic picture of the conformational changes induced upon Ca^{2+} binding. The rPCaM molecule assumes a dumbbell shape in the crystal and has a long central helix (residues 65–92) connecting the N- and C-terminal domains with two calcium-binding sites in each domain. Studies have shown that calmodulin activates protein kinases by binding to a peptide segment in the kinases and these peptides form amphiphilic α-helices (Lukas, Burgess, Pendergast, Lau & Watterson, 1986; Kemp, Pearson, Guerriero, Bagchi & Means, 1987). Recently, an X-ray (Meador, Means & Quiocho, 1992), NMR (Ikura *et al.*, 1992), and two modelling studies (Strynadka & James, 1990; Sekharudu & Sundaralingam, 1993*a*) of the calmodulin–MLCK (myosin light chain kinase) peptide complex have been reported, where the central helix is bent bringing the N- and C-terminal domains close together to encapsulate the helical peptide. Calmodulin has a highly conserved sequence, from *Paramecium* to human, and has about 148 residues and generally has a small number of di- or trimethylated lysine residues (Gregori, Marriott, Putkey, Means & Chau, 1987).

Our interest in *Paramecium* calmodulin (PCaM) was generated by the observation that various natural mutants of PCaM affect the behavior of the organism by affecting the Na^+/K^+ ion channels in *Paramecium* (Kink *et al.*, 1990). In order to understand its biological function, we plan to carry out X-ray structural studies to characterize the precise structural and conformational changes between PCaM and its mutants. We present here a detailed crystal structure determination and refinement at 1.68 Å resolution of recombinant *Paramecium* calmodulin (rPCaM). We also compare it with the wild-type PCaM and the two other known calmodulin structures; mammalian calmodulin (MCaM) and recombinant *Drosophila* calmodulin (rDCaM). The structures of both MCaM (Babu, Bugg & Cook, 1988; Babu *et al.*, 1985) and rDCaM (Taylor, Sack, Maune, Beckingham & Quiocho, 1991) have been determined to 2.2 Å resolution with an R value of 0.175 and 0.197, respectively. The wild-type PCaM has a di-methylated Lys13, a trimethylated Lys115 and an acetylated N-terminus (Gregori *et al.*, 1987; Kink, Maley, Ling, Kanabrochi & Kung, 1991), and has 18 sequence changes from MCaM and 17 changes from DCaM (Fig. 1). In the rPCaM expressed in *E. coli*, the post-translational modifications are absent. Previously we have reported the crystal structure of the wild-type PCaM at 1.8 Å resolution (Rao *et al.*, 1993). The present analysis of rPCaM at 1.68 Å resolution represents the highest resolution structure of a calmodulin determined to date with considerably more intensity data than the previous best X-ray study. This work defines the molecular geometry and structure very precisely and characterizes the extensive intra- and intermolecular hydrogen-bonding and hydration network in the crystal.

Material and methods

rPCaM

The calmodulin gene from *Paramecium tetraurelia* was expressed in *E. coli* and the protein was purified (Kink *et al.*, 1990, 1991). The protein was obtained in a solution containing 40 mM Tris buffer (pH 7.5), 50 μM EDTA, 2.4 M sucrose and 100 μg ml^{-1} of lysozyme. It was further purified with phenyl-Sepharose and HPLC chromatography. The *E. coli* expressed calmodulin (rPCaM) has the full sequence (residues 1–148).

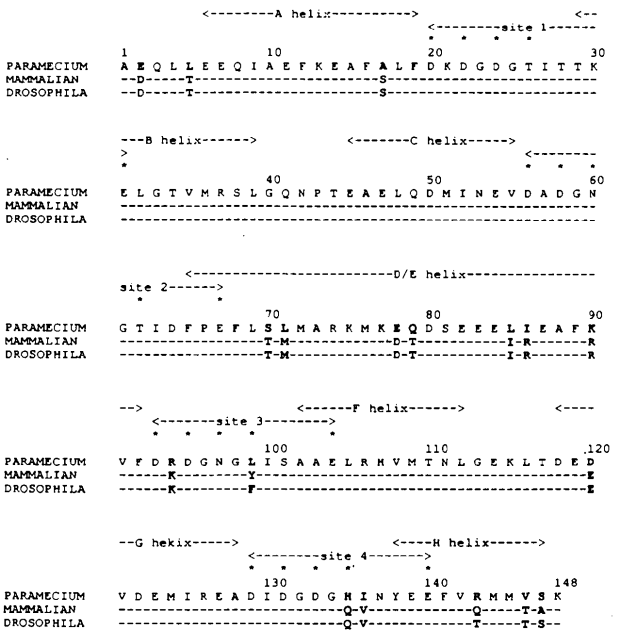

Fig. 1. Amino-acid sequence of calmodulins; the PCaM has 18 and 17 different residues compared to MCaM and DCaM, respectively. The different residues are indicated in bold type. The calcium-binding residues are marked by *.

Crystallization

Crystals of rPCaM were grown by the hanging-drop vapor-diffusion method at 277 K. The hanging drop contained 4.0 μl of unbuffered protein solution (15 mg ml^{-1}), 2.0 μl of 10 m*M* calcium chloride, 2.0 μl of 50 m*M* sodium cacodylate buffer (pH = 5.0) and 1.0 μl of 100%(*v*/*v*) 2-methyl-2,4-pentanediol. The reservoir solution was 1.0 ml of 50%(*v*/*v*) 2-methyl-2,4-pentanediol. The best crystals were obtained in about two weeks. They were rectangular in shape and formed clusters.

Data collection and reduction

A large crystal measuring 0.4 × 0.4 × 0.15 mm was mounted in an arbitrary orientation for data collection in a 0.7 mm Lindemann glass capillary with a little mother liquid at one end. The crystals were triclinic, with cell constants $a = 29.89$, $b = 53.42$, $c = 25.34$ Å, $\alpha = 93.67$, $\beta = 96.88$ and $\gamma = 89.24°$, space group *P*1 with one molecule in the unit cell. Three-dimensional X-ray intensity data to 1.68 Å resolution were collected at 263 K using an in-house Siemens–Nicolet area detector mounted on a four-circle goniometer. The X-ray source was a MaxScience 18 kW rotating Cu anode operated at 50 kV and 90 mA. A graphite monochromator was used to isolate the Cu $K\alpha$ radiation. The distance between the crystal and the area detector was 12.0 cm. A 360° φ scan at $\chi = 0°$ and eight ω scans at different φ and χ values were performed in 0.2° steps. A total of 4200 frames were collected, with an exposure time of 60 s frame^{-1}. The frames were processed using *XENGEN*1.3 software (Howard, Nielsen & Xuong, 1985). When the φ- and ω-scan data were merged, a total of 35939 reflections were obtained to yield 16255 unique reflections (92% of 17589 possible reflections) with an R_{symm} of 4.1%. In the 6.0–1.68 Å resolution range, there were 15965 unique reflections with $I > 1.5\sigma(I)$ and these were used in the refinement (Table 1).

Structure analysis and refinement

The atomic coordinates of the wild-type PCaM (Rao *et al.*, 1993) were used as the starting model containing four calcium ions and protein atoms for residues 5–147. The *X-PLOR* program package (Brünger, 1990) was used for the refinement. After rigid-body refinement, the *R* value dropped to 0.333 for data between 6.0 and 2.0 Å resolution. The first cycle of positional and *B* refinement reduced the *R* value to 0.293. At this point, all reflections [15965 reflections for $I \geq 1.5\sigma(I)$] were included from 6.0 to 1.68 Å resolution and omit $3F_o - 2F_c$ electron-density maps were calculated by omitting ten residues at a time. The omitted residues in each calculation were then refitted into the omit-density map using the *FRODO* program package (Jones, 1985) on an Evans and Sutherland PS340. After several alternating cycles of refinement and refitting the model, the *R* value was 0.263. In order to locate solvent molecules, difference electron-density maps were calculated. The potential sites were incorporated into the model if they appeared in both the $3F_o - 2F_c$ and $F_o - F_c$ (at heights $\geq 2.5\sigma$ above the mean) electron-density maps, and formed hydrogen bonds with correct geometry to either the polar protein atoms or other already established water molecules. In this way, 42 water molecules were located and included in the refinement and the *R* value dropped to 0.234. At this point, the electron-density maps showed clear densities for the N-terminal residues 1–4 (1-Ala-Glu-Gln-Leu-4) and the C-terminal residue Lys148 which were built and included in the model for further refinement. In the next round of refinement, 99 water molecules were included, the *R* value was 0.203. Several additional rounds of solvent selection, refitting the model and refinement were performed. Water molecules which had a *B* value greater than 60.0 Å^2 or $F_o - F_c$ density less than 2.5σ, were removed from the model. The model now has 1165 protein atoms (residues 1–148), four calcium ions, and 172 water molecules (Fig. 2). The final *R* value was 0.194 for 15965 reflections with $F \geq 3\sigma(F_o)$ in the resolution range 6–1.68 Å. The crystallographic parameters of the final refinement cycle are listed in Table 2. The atomic coordinates have been deposited with the Brookhaven Protein Data Bank* (Bernstein *et al.*, 1977).

Table 1. *X-ray intensity data of rPCaM*

Resolution range (Å)	Possible reflections	$I \geq 1.5\sigma(I)$ reflections	%
6.0–3.0	2760	2752	100
3.0–2.0	7491	7447	99
2.0–1.9	1785	1756	98
1.9–1.8	2202	1868	85
1.8–1.75	1274	1031	81
1.75–1.70	1451	843	58
1.70–1.68	626	269	43
Total	17589	15965	91

Results and discussion

Overall structure of rPCaM

The structure of rPCaM has been determined at higher resolution (1.68 Å) and with more data than any calmodulin structure reported so far (Table 3).

* Atomic coordinates and structure factors have been deposited with the Protein Data Bank, Brookhaven National Laboratory. Free copies mat be obtained through The Technical Editor, International Union of Crystallography, 5 Abbey Square, Chester CH1 2HU, England (Supplementary Publication No. SUP 37097). A list of deposited data is given at the end of this issue.

The crystal structure of rPCaM shows that it is generally similar to those of the other calmodulin structures. The final refined structure has very good stereochemistry with r.m.s. deviations of 0.012 Å and 2.4° for bond lengths and angles from ideality. The mean positional error (Luzzati, 1952) is 0.20 Å. The electron density over the entire molecule is generally very well defined. The side chains of Lys75, 77, Glu2

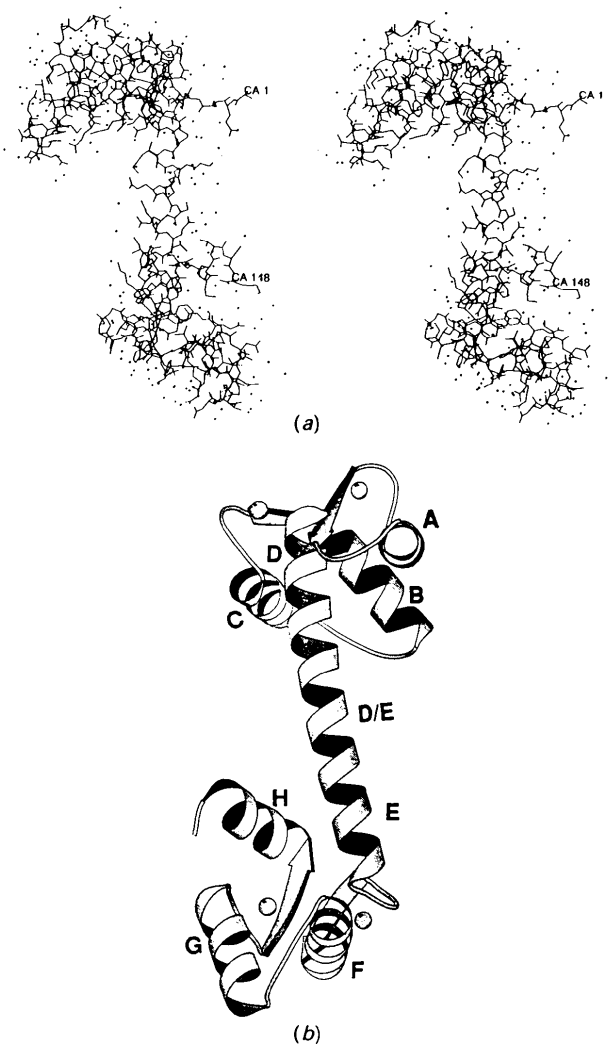

Fig. 2. (*a*) Stereoview of the refined rPCaM; all protein atoms, calcium ions and water molecules are included. View is selected in such a way that the curvature of the central helix is seen. (*b*) Ribbon diagram of rPCaM. The helical regions *A* though *H* are marked. The arrows indicate the β-sheets between the calcium-binding loops and the balls indicate Ca ions. View is similar to that shown for troponin C (Fig. 3, previous paper in this issue, Satyshur, Pyzalska, Rao, Greaser & Sundaralingam, 1994). Note that the N-terminal helix is absent in calmodulin, and the N-terminal domain has two Ca^{2+} ions and also the long central helix has 7.8 turns rather then 8.6 turns in troponin C. These differences are responsible for the different orientation of the N-terminal domains of the two molecules.

Table 2. *Summary of X-PLOR refinement parameters of the final model*

Resolution range (Å)	6.0 1.68
No. of reflections [$F \geq 3\sigma(F)$]	15 965
Final *R* value	0.194
Program	*X-PLOR*, version 2.1
R.m.s. deviation from ideal geometry*	
Bond lengths (Å)	0.012
Bond angles (°)	2.4
Dihedral angles (°)	23.2
'Improper' angles ( )	3.8
Parameter file used	param19.pro
Model	
Protein atoms (residues 1-148)	1165
Calcium ions	4
Water molecules	172

* The refinement terms in *X-PLOR* are restrained to equilibrium values by energetic force constants such that bond lengths are restrained for the vibration of two bonded atoms, bond angles for the bending of three bonded atoms, dihedral angles for torsional motions of four bonded atoms, and 'improper' angles for maintaining planarity and/or chirality of a group of atoms. The parameter file includes all of the equilibrium values and force constants necessary for restraints of the covalent bonds, bond angles, dihedral angles, and 'improper' angles. They were obtained from experimental spectroscopic data of small molecules.

Table 3. *Comparison of experimental data between rPCaM and other calmodulin structures*

	rPCaM	PCaM	MCaM‡	rDCaM‡
Number of residues	148	148	148	148
Sequence differences from PCaM		--	18	17
Unit-cell dimensions*				
a (Å)	29.89	29.66	29.71	29.57
b (Å)	53.42	53.79	53.79	53.92
c (Å)	25.35	25.49	24.99	24.78
α (°)	93.67	92.84	94.13	97.08
β (°)	96.88	97.02	97.57	97.09
γ (°)	89.24	88.54	89.46	88.86
Space group, *Z*	*P*1, 1	*P*1, 1	*P*1, 1	*P*1, 1
Resolution range (Å)	6 1.168	10 1.8	5–2.2	10–2.2
No. of reflections	15965	11458	6685	5239
Final *R* value†	0.194	0.210	0.175	0.197
Final model				
Protein residues	1 148	4 147	5–147	1 148
Ca^{2+} ions	4	4	4	4
Water molecules	173	71	69	78
R.m.s. in bond lengths (Å)	0.012	0.016	0.016	0.018

* The *a* and *b* cell dimensions show smaller differences, but *c* is significantly longer than in MCaM and rDCaM. The α angle shows the largest difference compared to rDCaM.

† In rPCaM refinement, higher resolution and more data were used than in other calmodulins and the covalent bonds have a lower r.m.s. (0.12 Å) than in other CaM's.

‡ The atomic coordinates of MCaM (3CLN) and rDCaM (4CLN) were from the Brookhaven Protein Data Bank (Bernstein *et al.*, 1977).

and a carboxyl O atom of Lys148 show weak electron density ($<1\sigma$ in the difference maps). The electron density is discontinuous for the side chains of Lys30, Glu54 and Glu83. These residues have high temperature factors (Fig. 3). The average *B* parameter is 19.8 Å^2 for all atoms and 21.4 Å^2 for the backbone atoms. The central helix region exhibits a high *B* factor throughout, though not as high as the N- and C-termini. The average *B* value for the N-terminal residues 1–5 is 45.2 Å^2, for the C-terminal residues 144–148 is 51.2 Å^2, and for the central helix residues 65–92 is 27.2 Å^2. The high *B*

values are expected for the free termini, but the relatively high *B* values for the central helix atoms are probably due to the fact that they are generally exposed to the aqueous environment, even though some of the central helix residues are involved in intermolecular hydrogen bonding. The rPCaM structure is a dumbbell-shaped molecule, with seven α-helices [*A* helix (6–19), *B* helix (29–39), *C* helix (45–55), *D/E* helix (65–92), *F* helix (102–111), *G* helix (118–128) and *H* helix (138–147)] including a long 7.8 turn central helix (*D/E* helix) connecting the two terminal domains.

N- *and* C-*terminal residues*

The four N-terminal residues which are non-helical, stretch out from the *A* helix and make intermolecular contacts with a neighboring molecule (Fig. 40. The backbone amide N atom of Ala1 is involved in a water bridge with the NE2 atom of Glu79 of a neighboring molecule. The carboxylate O atom of Glu2 forms a salt bridge with the side chain of Lys90 ($d = 3.0$ Å) of a neighboring molecule. In the 2.2 Å resolution structure of rDCaM (Taylor *et al.*, 1991), the N-terminal residues have a different conformation curving towards the second calcium-binding site, with Asp2 making a close contact with Leu69 (see note below). However, in MCaM (Babu *et al.*, 1988) and wild-type PCaM (Rao *et al.*, 1993), the first four residues of the amino-terminal end are not visible in the electron-density map. In the present rPCaM the electron density for the C-terminal Lys148 was very clear but one of the terminal carboxyl O atoms had no density (Fig. 4). The C-terminal end is stabilized by a series of interactions with the long central helix of a neighboring molecule. The side chain of Lys148 forms an internal salt bridge with the side chain of Glu87 ($d = 2.7$ Å) of a neighboring molecule. The carbonyl O atom of Ser147 and a carboxylate O atom of Lys148 are bridged by water molecules to the OE2 atom of Glu83 of a symmetry-related molecule.

Structure of the calcium-binding sites

The *EF*-hand is a helix–loop–helix super-secondary structural domain that binds a calcium ion in the 12-residue loop and was first identified in the crystal structure of parvalbumin where the two *EF*-hands are related by an approximate twofold axis (Kretsinger & Nockolds, 1973). In rPCaM, each terminal domain contains a pair of '*EF*-hands' where the Ca^{2+} ions are bound. The four Ca^{2+}-binding loops in these *EF*-hands are site 1 (20–31), site 2 (56–67), site 3 (93–104) and site 4 (129–140), flanked by helices on either side (Fig. 2).

Conformational similarities and differences amongst the four loops. In the crystal structure of rPCaM, the sites 1 and 3 are most similar (r.m.s. = 0.31 Å) and sites 1 and 4 are least similar (r.m.s. = 0.79 Å) (Table 4). Site 4 has the highest r.m.s. deviation compared to other sites. The superposition of the four calcium-binding sites is shown in Fig. 5. The largest deviations are seen between site 4 and the other sites particularly at the first and the ninth to twelfth positions in the loops. The ninth and tenth positions form the mini β-sheet and may be more flexible because of the bridging water molecules extending the β-sheet (see below). Indeed these residues show the highest r.m.s. deviations. The interhelical angle at site 4 (116°) is more obtuse than at the other sites 1, 2 and 3 of 99, 96 and 102°, respectively. Thus, there are some apparent conformational differences between site 4 and the other sites.

Calcium coordination by the loops. All four calcium ions in the 12-residue loops of rPCaM are seven coordinated (Table 5). The coordination involves the side-chain carboxylate O atoms of the first, third and fifth residues, the backbone carbonyl O atom of the seventh residue, both the carboxylate O atoms of the glutamic residue at the twelfth position and a water molecule. The average coordination distances to the calcium ions in the four sites are in the range 2.30–2.39 Å, similar to that found for seven-coordinated calcium complexes (Einspahr & Bugg, 1984).

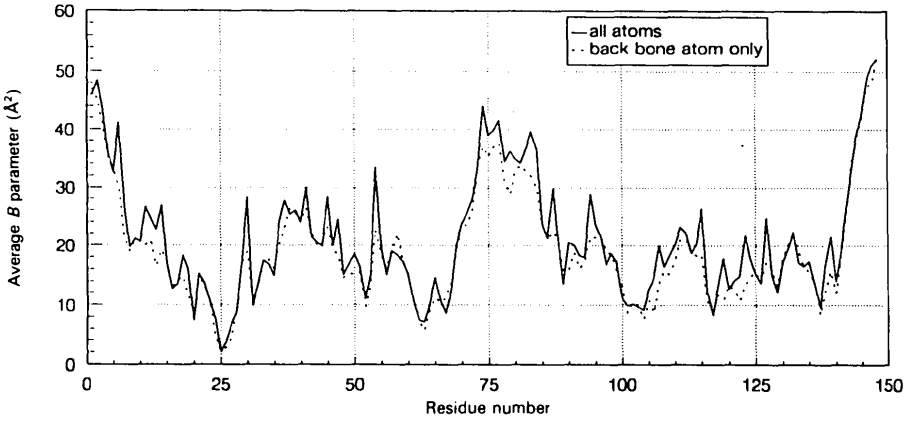

Fig. 3. Average thermal *B* parameters for main-chain and all atoms ($\langle B\rangle_{\text{main-chain}} = 19.7$ Å^2 and $\langle B\rangle_{\text{all atoms}} = 21.4$ Å^2). The solid line is for all atoms and the dotted line is for backbone atoms.

Stabilization of the loops by hydrogen bonds. The calcium-binding loops are stabilized by a series of hydrogen bonds between residues 1–4, 3–12 and 9–12 as found in other *EF*-hands (Strynadka & James, 1989). In rPCaM, additional hydrogen bonds are found; the backbone NH group at the twelfth residue of the loops forms hydrogen bonds with the side chains of the ninth residue, while the side chains of the twelfth residue form hydrogen bonds with the backbone amide of the fourth residue. The backbone and side-chain O atoms of the first residue also form hydrogen bonds to the backbone amide and side-chain O atom of the fifth residue, respectively, except for site 4, where this hydrogen bond is not observed. This is because the conformational changes in the backbone at site 4 are too large to permit the formation of the hydrogen bond. The last three residues of the calcium-binding loops are in the second helix of the *EF*-hands.

Table 4. *R.m.s. deviations* (Å) *between the four* Ca^{2+}-*binding sites*

The upper triangle contains the r.m.s. deviations for the backbone atoms and the lower triangle for the C$^{\alpha}$ atoms.

	Site 1	Site 2	Site 3	Site 4
Site 1 (residues 20–31)		0.47	0.31	0.79
Site 2 (residues 56–67)	0.41	—	0.41	0.52
Site 3 (residues 93 104)	0.28	0.37	—	0.72
Site 4 (residues 129 140)	0.71	0.42	0.63	—

Hydration of the calcium-binding loops. The water molecules in sites 1 and 3 that are involved in coordination with the Ca^{2+} ions also form hydrogen bonds to the side-chain O atoms of the seventh residue. In site 2, the water molecule is hydrogen bonded to the carboxylate O atom of the ninth residue while in site 4, the water molecule forms a hydrogen bond with the side chain of the twelfth residue. The water molecules in sites 1, 2 and 3 (but not 4) in turn are hydrogen bonded to a second water molecule. In addition, the water molecule in site 1 makes an intermolecular hydrogen bond with OD1 of Asp118 of a symmetry-related molecule. Thus, besides many similarities, there are small differences in the first shell hydration of the four calcium-binding sites.

Differences in the calcium-binding sites – relationship to their affinities. In calcium-binding proteins such as calmodulin and troponin C, the functional *EF*-hands that bind Ca^{2+} always seem to occur in pairs (Sekharudu & Sundaralingam, 1988). Both *EF*-hand pairs of the N- and C-terminal domains of calmodulin bind two Ca^{2+}, [$pK_d(Ca^{2+}) \simeq 6.5$], or

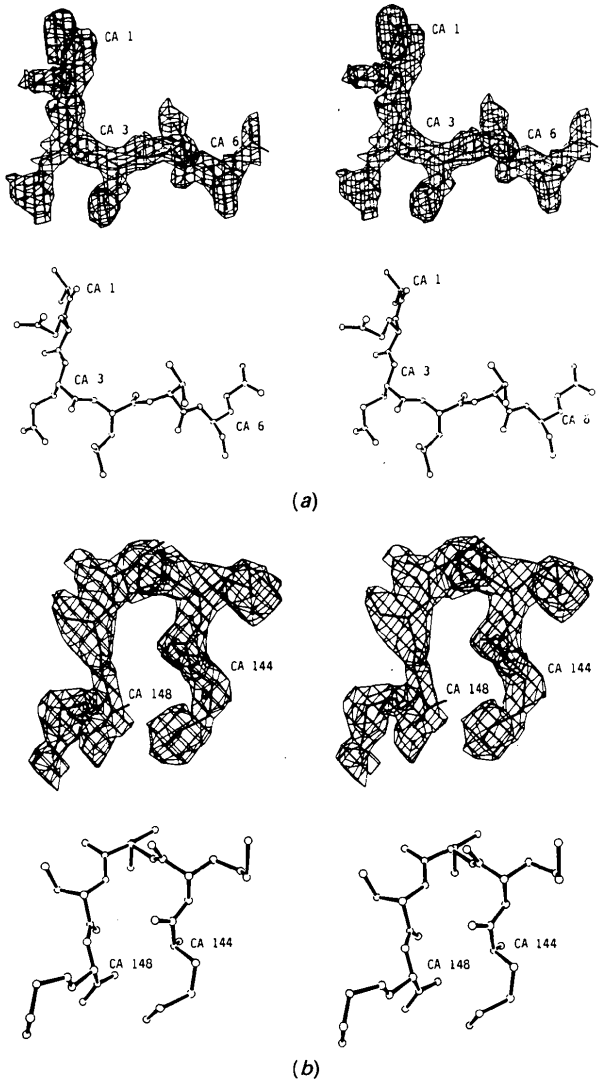

Fig. 4. Stereoviews of the omit $3F_o - 2F_c$ electron-density map ($> 1.2\sigma$) for (*a*) the N-terminal, six residues 1–6, with a ball-and-stick plot in the same view, (*b*) for the C-terminal five residues 144–148, with a ball-and-stick plot in the same view. See Fig. 6 for better electron density for a segment.

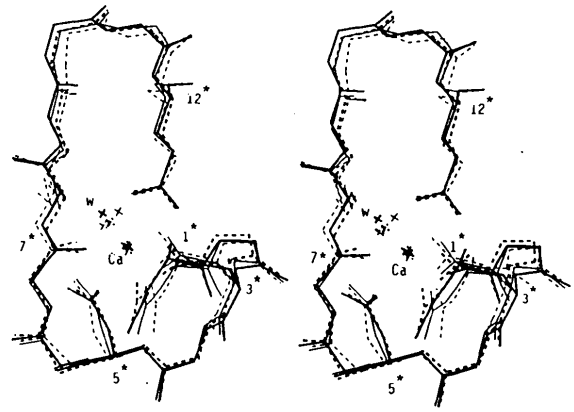

Fig. 5. Stereoview of the superposition of the four calcium-binding sites; the thick solid line indicates site 1, thin solid line site 2, thick dotted line site 3, and thin dotted line site 4.

Table 5. *Calcium-ion coordination at the four sites in rPCaM*

Site 1		Site 2		Site 3		Site 4	
Atom	Distance (Å)	Atom	Distance (Å)	Atom	Distance (Å)	Atom	Distance (Å)
OD1-D20	2.35	OD2-D56	2.23	OD2-D93	2.24	OD1-D129	2.04
OD1-D22	2.47	OD2-D58	2.20	OD2-D95	2.38	OD1-D131	2.14
OD2-D24	2.30	OD1-N60	2.32	OD1-N97	2.42	OD2-D133	2.21
O-T26	2.12	O-T62	2.19	O-L99	2.13	O-H135	2.34
OE1-E31	2.54	OE1-E67	2.43	OE1-E104	2.37	OE1-E140	2.47
OE2-E31	2.40	OE2-E67	2.58	OD2-E104	2.52	OE2-E140	2.69
*W*153	2.58	*W*157	2.24	*W*189	2.37	*W*181	2.21
Average	2.39		2.31		2.35		2.30
R.m.s.	0.16		0.14		0.13		0.22

other divalent cations, with high affinity although the calcium-binding sites in the C-terminal domain have slightly higher cation affinity than the N-terminal domain (Cox, Corute, Mamar-Bachi, Milos & Schaer, 1988). In troponin C, the C-terminal domain has two orders of magnitude higher affinity for Ca^{2+} compared to the N-terminal domain (Wnuk, 1988). The crystal structure of troponin C (pH 5.1) demonstrates this by not binding Ca^{2+} in the two low-affinity *EF*-hand motifs of the N-terminal domain while binding Ca^{2+} in the two high-affinity *EF*-hand motifs of the C-terminal domain (Satyshur *et al.*, 1988; Herzberg & James, 1988). The differences in the affinities of the paired *EF* motifs in troponin C can be rationalized by the sequence differences between the N- and C-terminal domains (Sekharudu & Sundaralingam, 1988). On the other hand, in calmodulin, the apo (metal-free)

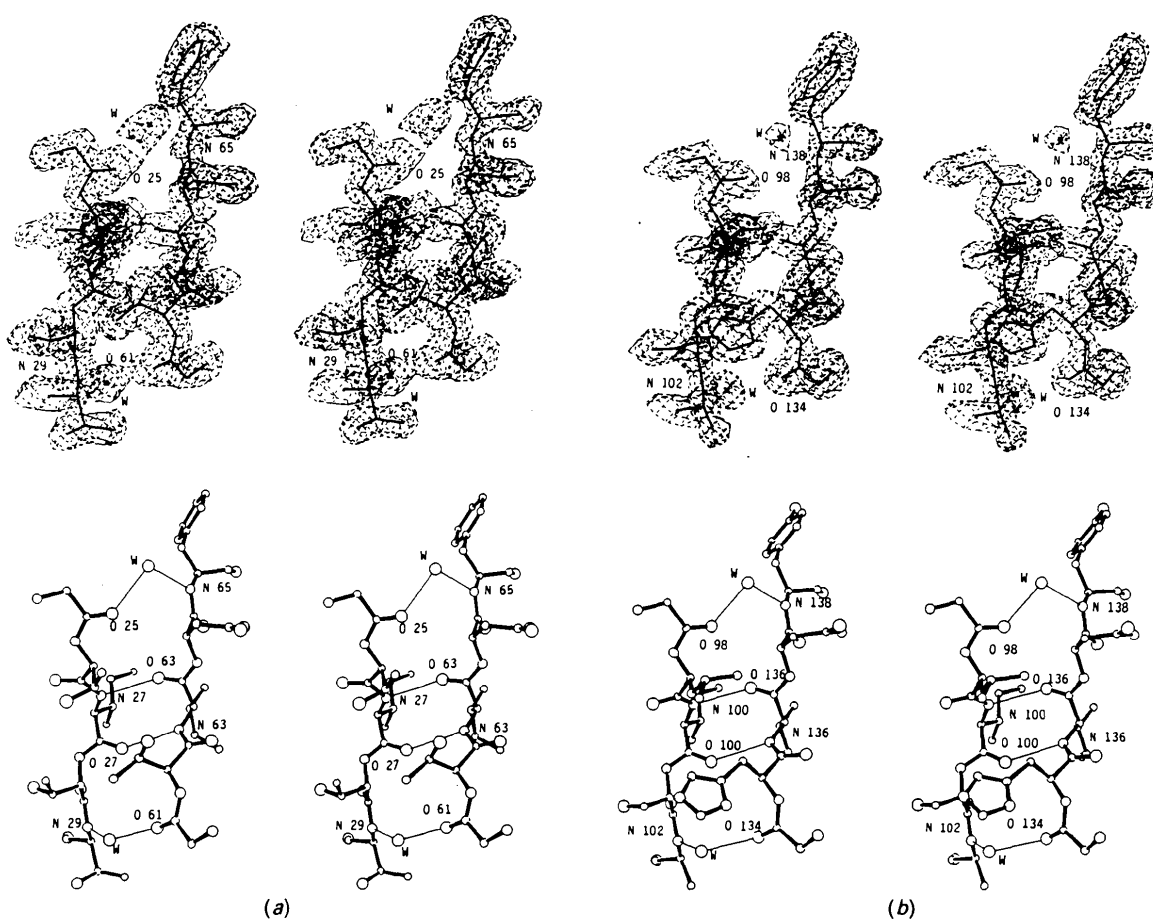

Fig. 6. (*a*) Stereoview of the mini β-sheet between the calcium-binding loops 1 and 2. Top, omit $3F_o - 2F_c$ electron-density map ($> 1.5\sigma$), and bottom, a ball-and-stick plot. Note the two water-bridged β-sheet hydrogen bonds on either sides of the β-sheet hydrogen bonds. (*b*) Stereoview of the mini β-sheet between calcium-binding loops 3 and 4. Top, omit $3F_o - 2F_c$ electron-density map ($> 1.5\sigma$), and bottom, a ball-and-stick plot.

EF-motif is not found because the sequences of the two domains are more similar and their binding affinities are comparable.

Mini β-sheets stabilize the pair of calcium-binding sites. The helix–loop–helix (*EF*-hand) motifs are further stabilized by a series of β-strand pairs between the eighth residues of adjacent loops. The Ca^{2+}-binding loops of the *EF*-hand motifs form a short stretch of antiparallel β-sheet. In the N-terminal domain, residue Ile27 in site 1 forms a pair of β-sheet hydrogen bonds with Ile63 of site 2, and in the C-terminal domain, residue Ile100 in site 3 forms a pair of β-sheet hydrogen bonds with Ile136 of site 4. These pairs of mini β-sheets in each domain are further extended by water bridges between the N—H and C=O groups on either sides of the mini β-sheets (Fig. 6). The extended water-bridged β-sheet was first observed in the holo C-terminal domain of chicken skeletal muscle troponin C (Satyshur *et al.*, 1988, and unpublished results). The importance of these water-bridged β-sheets in the initial formation and unfolding of the β-sheets has been recognized (Sekharudu & Sundaralingam, 1993*b*).

Structural differences between the N- *and* C-*terminal domains*

The 62 C^{α} atoms of the N-terminal domain (residues 11–73) and the C-terminal domain (residues 84–146) have an r.m.s. deviation of 0.74 Å with the first four residues in the linker regions (residues 39–42 and 112–115) having the highest r.m.s. deviation (average 1.32 Å) (Fig. 7). In this comparison, the amino-acid sequences of the N- and C-terminal domains reveal that 28 residues are indentical, 26 residues are conservatively changed, and nine residues are different. Although the side chains of the nine residues are different, they have quite similar intra- and intermolecular interactions. Only two of these nine residues form water bridges. The side chain of Thr26 in calcium-binding site 1 is bridged to Asp24 through one water molecule and to Thr62 in calcium-binding site 2 through two water molecules.

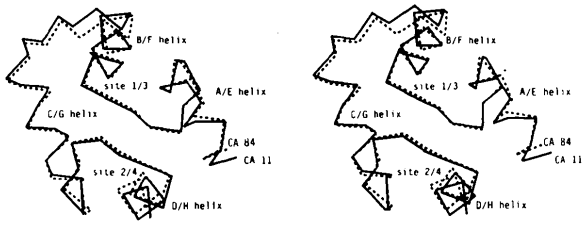

Fig. 7. Stereoview of the superposition of the corresponding C^{α} atoms of the N- and C-terminal domains. The solid line indicates the N-terminal domain (residues 11–73) and the dotted line indicates the C-terminal domain (residues 84–146).

Similarly, in the C-terminal domain the side chain of Asp106 also forms a water bridge to the side chain of Asp118. Lys90 forms a salt bridge with the side chain of Glu2 while the Glu139 side-chain forms a direct intermolecular hydrogen bond with the side chain of Glu6. Both of these hydrogen bonds are to two different neighboring molecules. Also, an additional salt bridge is formed between the side chains of Glu139 and Arg143 (d = 2.7 Å).

Central α-helix

The 28 residues of the central helix (residues 65–92) in calmodulin form nearly a 7.8-turn α-helix, spanning the two terminal domains, thus giving a dumbbell shape to the protein. In the crystal structure of rPCaM, the main-chain α-helical atoms, particularly those of the *D/E* linker region (residues 73–84), have relatively higher B parameters (Table 6) (Fig. 3). This is because the segment is more exposed and flexible in accord with the tryptic cleavage of calmodulin in the presence of Ca^{2+} ions which occurs preferentially in the *D/E* linker region (Newton, Oldewurtel, Krinks, Shiloach & Klee, 1984; Persechini & Kretsinger, 1988). Also the flexibility of the central helical region is demonstrated by the nearly linear X-ray structure for calmodulin on one hand and the highly bent calmodulin in the calmodulin–peptide complex (Meador *et al.*, 1992; Ikura *et al.*, 1992; Strynadka & James, 1990; Sekharudu & Sundaralingam, 1993*a*) on the other. Nearly all the backbone carbonyl O atoms of the solvent-exposed central α-helix region (residues 73–84) are hydrogen bonded to the surrounding water molecules as in wild-type PCaM (Rao *et al.*, 1993). This feature was again first seen in troponin C (Satyshur *et al.*, 1988). In addition, the N-terminal α-helix of the central helix displays three intra-helical water bridges between the carbonyl O atom of Glu67 and the hydroxyl group of Ser70, the carbonyl O atom of Ser70 and the amide N atom of Arg74, and the carbonyl O atom of Arg74 and the side-chain carboxylate O atom of Glu78 (Fig. 8). All of these water bridges occur around the top half of the long helix.

Normally a single solvent molecule interacting with a carbonyl group of an α-helix can cause a kink or bend in the helix (Blundell, Barlow, Borkakoti & Thornton, 1983; Sundaralingam & Sekharudu, 1989). The eight backbone carbonyl O atoms of the central helix in rPCaM that are hydrogen bonded to water molecules nearly surround the long helix and a marked bend is not observed (Table 7). The carbonyl groups of the residues that are hydrated, Pro66, Glu67, Leu69, Ser70, Arg74, Ser81, Glu84 and Lys91 are shown in Fig. 8. Additionally, the carbonyl O atoms of Lys77 and Glu78 of the long helix make

Table 6. *Hydrogen-bonding, backbone torsion angles and B values of the central α-helix of rPCaM*

Residue (*i*)	$O_i\cdots N_{i+4}$ distance (Å)	$C{=}O_i N_{i+4}$ angle (°)	φ (°)	ψ (°)	$\langle B_i \rangle$ (Å^2)
F65	2.9	162.6	−75	−41	14.7
F66	3.2	152.6	−52	−40	10.7
E67	3.3	148.0	−69	−36	8.7
F68	3.0	153.4	−75	−33	12.6
L69	3.2	149.9	−63	−45	20.3
S70*	3.2	151.9	−52	−50	23.6
L71	3.0	164.3	−57	−53	25.5
M72†	3.1	149.9	−62	−30	28.0
A73†	3.1	154.1	−71	−52	33.0
R74	3.0	154.6	−57	−48	44.1
K75	2.9	153.8	−59	−49	39.0
M76	3.0	149.9	−72	−52	39.8
K77	3.3	155.8	−63	−47	41.6
E78	3.1	151.7	−62	−38	34.4
Q79	3.1	149.4	−72	−28	36.2
D80	3.1	164.9	−66	−56	34.9
S81	3.3	146.6	−60	−27	34.1
E82	3.0	156.8	−72	−34	36.6
E83	3.0	150.5	−63	−42	39.6
E84†	2.9	155.9	−60	−52	36.5
L85†	3.1	147.4	−61	−38	23.9
I86	3.1	147.0	−67	−37	21.3
E87	3.3	151.0	−67	−44	29.8
A88	3.3	152.6	−69	−35	20.6
F89	–	–	−62	−43	13.6
K90	—	—	−72	−22	20.6
V91	—	—	−73	−42	20.1
F92	—	—	−66	−38	18.3
Range	2.9–3.3	146.6–162.6	−52–−75	−27–−56	8.7–44.1
Mean	3.1	153.1	−65	−41	27.2
R.m.s.	0.13	6.2	6.5	8.7	10.3

* The carbonyl O atom of Ser70 and the amide N atom of Arg74 are also bridged by two water molecules.

† Ala74 to Glu84 which have relatively higher *B* values lie between these residues.

bifurcated hydrogen bonds with the side chain of Ser81. The φ, ψ torsion angles of the long helix are distorted by a decrease in the $C{=}O_i N_{i+4}$ angles and an increase in the $O_i\cdots N_{i+4}$ distances (Blundell *et al.*, 1983) since most of the carbonyl O atoms are involved in hydrogen bonding to water molecules. The mean $O_i\cdots N_{i+4}$ distance and $C{=}O_i N_{i+4}$ angle for the nine carbonyl to water hydrogen bonds are 3.2 Å and 151.8°, respectively (Table 7). The corresponding distance and angle values for the remaining carbonyl groups of the long helical region not involved in hydrogen bonding to an external solvent molecule are 3.1 Å and 153.8°. This confirms the hypothesis of Blundell *et al.* (1983) that the binding of a water molecule to a helix backbone carbonyl O atom weakens the helix hydrogen bond.

Hydration and crystal packing

A total of 172 ordered water molecules (about 30% of the water molecules in the unit cell) were located in the crystal structure. Of these 131 are in the first coordination shell, directly hydrogen bonded to protein atoms. The remaining 41 water molecules interact with the protein *via* water bridges. 34 water molecules take part in forming intramolecular water bridges (Table 8); 14 between side-chain atoms, 14 between side-chain and backbone atoms, and 11 between backbone atoms, including four water molecules in the mini anti-parallel β-sheets. A water molecule bridges the carbonyl O atom of Val55 which is the last residue of the *C* helix and the carbonyl O atom of Glu67 which is the last residue of the calcium-binding loop 2, forming a pseudo-cyclic structure for the loop (Fig. 9). A similar hydrogen bonding is observed in C-terminal domain, where the corresponding carbonyl O atoms of Ala128 and Glu140 are also bridged by a water molecule. There are no such water bridges in the calcium-binding sites 1 and 3.

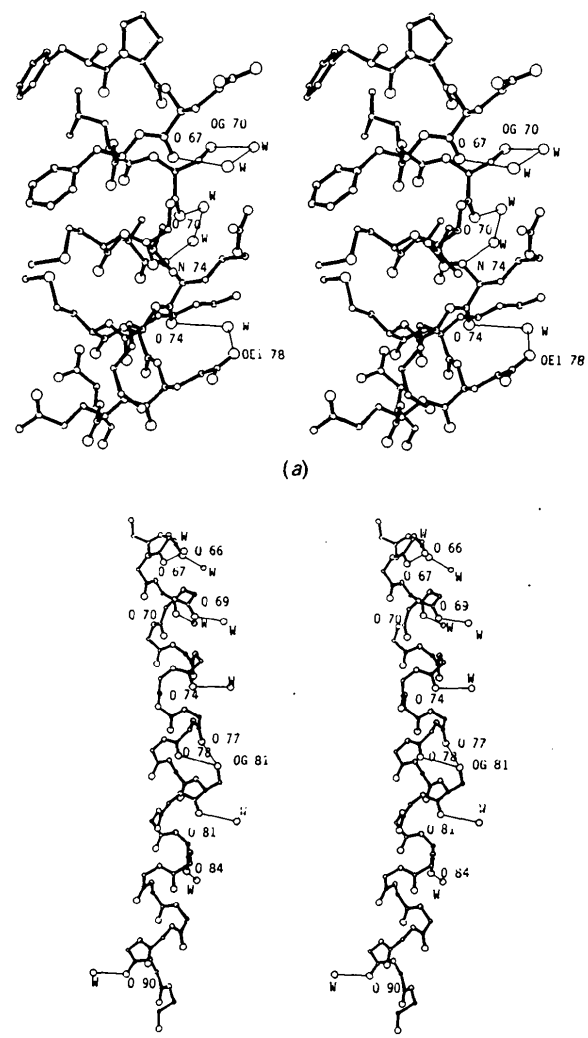

Fig. 8. Stereoviews showing (*a*) the water bridges with the side chains and (*b*) the hydrogen-bonded carbonyl O atoms to water molecule in the central α-helix. The helix is projected onto the plane of curvature. Note that the water molecules are generally located on one side of the helix.

Table 7. *External hydrogen bonding of the central α-helix carbonyl O atoms to side-chain atoms and surrounding water molecules in rPCaM*

Carbonyl of residue (*i*)	Distance (Å)	Atom 2/ residue	$O_i \cdots N_{i+4}$ distance (Å)	$C{=}O_i N_{i+4}$ angle (°)
O—P66	2.9	*W*217	3.2	152.6
O—E67	2.8	*W*159	3.3	148.0
O—L69	2.7	*W*255	3.2	149.9
O—S70	2.6	*W*218	3.2	151.9
O—R74	3.3	*W*322	3.0	154.6
O—K77	3.4	OF—S81	3.3	155.8
O—E78	3.4	OF—S81	3.1	151.7
O—S81	3.2	*W*261	3.3	146.6
O—E84	2.7	*W*180	3.0	155.9
O—K90	3.1	*W*270	—	—
O—V91	2.7	NH2—R126*		
		Average	3.2	151.8
		R.m.s.	0.13	5.09

* Of a *c*-axis translated molecule.

There are 15 direct intermolecular hydrogen bonds in the rPCaM crystal structure, and of these residues, Glu2, Lys21, Arg37, Glu87 and Arg94 form intermolecular salt bridges with Lys90, Asp50, Glu114, Lys148 and Asp119 of the neighboring molecules, respectively (Table 9). 30 water molecules are involved in the intermolecular water bridges (Table 10), and they are between (1) the *A* helix and the last *EF*-hand motif in the C-terminal domain; (2) the calcium-binding site 1 and the *C* and *G* helices of different molecules; (3) the *B* helix and the linker region (*F*/*G*) in the C-terminal domain; (4) the *G* helix and both linker regions (*B*/*C* and *F*/*G*) of the N- and C-terminal domains; and (5) the central long helix and the N-terminus and the C-terminus of neighboring molecules. The hydrophobic residues of rPCaM form the familiar hydrophobic patches in the two palms and are not in contact with neighboring molecules to yield any intermolecular hydrophobic interactions in the crystal.

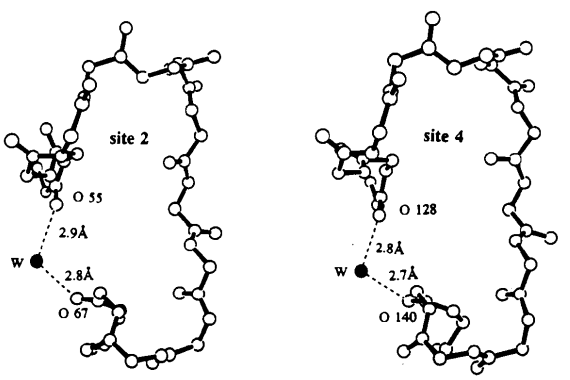

Fig. 9. Pseudo-cyclization of the calcium-binding loops 2 and 4. Shown are the bridging water molecules between carbonyl groups of residues Val55 and Glu67 in site 2 (left) and the residues Ala128 and Glu140 of site 4 (right). Such water bridges are not found in sites 1 and 3.

Table 8. *Intramolecular water bridges in rPCaM*

Atom 1/ residue	Distance 1 (Å)	Water 1	Distance 2 (Å)	Water 2	Distance 3 (Å)	Atom 2/ residue
Backbone–backbone atoms						
O V55	2.9	*W*159	2.8			O-E67
N-A102	2.9	*W*160	2.8			O-G134
O A128	2.8	*W*161	2.7			O-E140
N-Y29	2.8	*W*166	2.6			O-G61
O-G98	2.7	*W*174	3.0			N-Y138
O-G25	2.8	*W*194	2.8			N F65
O S70	2.6	*W*218	2.8	*W*237	3.1	N-R74
O R106	3.1	*W*221	2.5			O E114
			2.8			N-L116
O-K90	3.1	*W*270	3.1			O-D93
O R143	2.9	*W*320	2.9			O-S147
Backbone side-chain atoms						
O-E67	2.8	*W*159	2.6	*W*253	3.3	OF-S70
O-G61	2.8	*W*164	2.5	*W*251	2.9	NE2-Q49
N-T29	2.8	*W*166	2.9			
O-D119	2.8	*W*177	2.8			NH1-R126
O A46	2.6	*W*195	2.6			OD2-D50
O-N60	2.6	*W*202	2.7	*W*199	3.0	OG1-T62
O-L112	3.2	*W*288	3.1			OE2-E114
O Q3	2.9	*W*312	2.9			NE2-Q8
O-R143	2.9	*W*320	3.0			OG1 T146
O-S147	2.9					
O-R143	3.0	*W*321	2.7			OT2-K148
O R74	3.3	*W*322	2.7			OE1 E78
Side-chain–side-chain atoms						
NH1-R106	2.7	*W*154	3.1			OD2-D118
ND2 N53	3.0	*W*155	2.8			OD1 D56
OE2-E67	2.7	*W*158	2.7	*W*246	2.6	OD1-D64
OE2-E45	2.7	*W*167	3.0			NE2 Q49
OD2-D118	3.0	*W*176	2.8	*W*282	2.6	OD1-D122
OD1-D119	2.6	*W*177	2.8			NH1-R126
OD1 D24	3.2	*W*183	3.0			OG1-T26
			2.7	*W*199	3.0	OG1-T62
OE1-E139	2.6	*W*139	2.7			NH1-R143
ND2-N60	3.1	*W*201	2.6			OG1 T62
OG1-T110	2.7	*W*216	2.8			ND2 D111
OD2-D50	3.1	*W*232	3.1			OD1 N53

Table 9. *Intra- and intermolecular salt bridges and shorter intermolecular interactions in rPCaM*

Atom 1/residue	Distance (Å)	Atom 2/residue	Translation	Remarks
Intramolecular salt bridges				
NH1-R106	3.4	OD2-D118		Salt bridge*
OE1-E139	2.7	NH1-R143	—	Salt bridge
Intermolecular interactions				
OE1 E2	3.0	NZ-K90	−1, 0, 0	Salt bridge
N-E6	2.7	OE2 E139	−1, 0, 1	
NZ-K21	3.3	OD2-D50	0, 0, 1	Salt bridge
O-D22	2.6	NH2-R106	−1, 1, 1	
OD1-D24	3.0	N-D118	−1, 1, 1	
OG1-T34	2.7	OE2-E114	0, 1, 1	
NE-R37	3.0	OE1-E114	0, 1, 1	Salt bridge
NH2-R37	2.7	OE1-E114	0, 1, 1	
ND2-N42	2.8	O-K115	0, 1, 1	
	3.1	OE2-E120	0, 1, 1	
OE2-E87	2.7	NZ K148	0, 0, 1	Salt bridge
O-K90	2.9	NE-R126	0, 0, 1	
O-V91	2.7	NH2-R126	0, 0, 1	
NZ-K90	3.0	O-D129	0, 0, 1	
NH2-R94	2.9	OD1-D119	0, 0, 1	Salt bridge

* The term salt bridge indicates a direct hydrogen bond or ion pair.

Comparison with other calmodulin structures

We have compared our structure with those of wild-type PCaM (Rao *et al.*, 1993), MCaM and rDCaM. The r.m.s. deviation between rPCaM and wild-type PCaM is 0.36 Å for the equivalent C^{α} atoms (residues 4–147). The wild-type PCaM has a di-methylated Lys13, a tri-methylated Lys115, and

Table 10. *Intermolecular water bridges in rPCaM*

Atom 1/residue	Distance 1 (Å)	Water 1	Distance 2 (Å)	Water 2	Distance 3 (Å)	Atom 2/residue	Translation
OE2-E47	2.8	*W*156	2.9			OD1-D118	−1, 1, 1
O-A128	2.8	*W*161	2.8	*W*271	2.7	O-A1	1, 0, 0
O-E140	2.7						
O-T34	2.7	*W*163	2.9			O-G113	0, 1, 1
			3.1			N-K115	0, 1, 1
OD1-N42	2.6	*W*169	3.3			O-G25	1, 0, 0
O-A17	2.6	*W*173	2.8			OD2-D50	0, 0, 1
N-N42	2.7	*W*175	3.0			OD1-D64	1, 0, 0
O-T110	2.8	*W*178	2.6	*W*285	2.7	O-D58	1, −1, 0
O-E84	2.7	*W*180	3.1	*W*186	2.7	OE1-E127	0, 0, 1
N-E7	3.3	*W*182	2.6			OE1-E127	−1, 0, 1
OG1-T117	2.6	*W*190	2.8	*W*199	3.0	OG1-T62	1, −1, −1
O-L4	2.6	*W*191	2.6			OE1-E139	−1, 0, 1
			2.7			NH1-R143	−1, 0, 1
O-D24	2.7	*W*198	2.6	*W*293	2.7	O-R37	0, −1, −1
					2.6	OD1-N42	0, −1, −1
NH1-R37	2.9	*W*206	2.8			OE1-E120	0, 1, 1
N-A46	3.1	*W*213	2.9			O-N111	0, 1, 0
O-G59	3.3	*W*215	2.9			O-G23	0, 0, −1
			3.0	*W*298	3.2	NH2-R106	1, −1, 1
OD1-D119	2.7	*W*222	2.9			NH2-R94	0, 0, −1
O-R126	2.8	*W*223	2.8	*W*239	2.6	OE2-E2	1, 0, −1
			3.2	*W*270	3.1	O-K90	0, 0, −1
					3.1	O-D93	0, 0, −1
O-K21	2.6	*W*232	3.1			OD2-D50	0, 0, 1
NE-R74	3.0	*W*236	3.3			OE1-E14	0, 0, −1
NH2-R74	2.8						
OE2-E2	2.6	*W*239	3.0			O-D129	−1, 0, 1
OD1-D58	2.6	*W*254	3.3			OE2-E47	−1, 0, 0
NE2-E79	2.8	*W*271				N-A1	1, 0, 0
NZ-K115	3.1	*W*285	2.7			O-D58	1, −1, 0
O-I130	2.7	*W*312	2.9			O-E3	1, 0, −1
NE2-N8	2.9						
O-S147	3.0	*W*321	3.0			OE2-E83	0, 0, −1
OT2-K148	2.7						
NZ-K115	2.5	*W*325	3.1			O-A57	0, 0, 1

Table 11. *Torsion angles and intermolecular interactions of Lys*13 *and Lys*115 *in rPCaM and wild-type PCaM*

	Torsion angles (°)						Intermolecular interaction			
	φ	ψ	χ_1	χ_2	χ_3	χ_4	Atom 1	Distance (Å)	Atom 2	Translation
Recombinant										
K13	−62	−37	−54	−158	−58	178	NZ	2.5	Water	
K115	−86	−102	−45	−159	145	−92	NZ	2.7	Water	
							NZ	3.3	O-D58	1, −1, 0
Wild type										
K13	−59	−44	−142	−17	−179	−57	NZ*	2.9	Water	
K115	−91	−104	−83	−162	−177	175	NZ†	- -	—	

* Di-methylated.
† Tri-methylated.

an acetylated N-terminus resulting from post-translational modification. The backbone atoms of Lys13 and Lys115 in both structures have no significant differences; however, the side-chain conformations are quite different (Table 11). In the wild-type PCaM, the side chains of Lys13 and Lys115 are bent into the interior of the molecule, in contrast, the corresponding unmodified Lys residues in rPCaM stretch out into the solvent. The extended conformation of Lys113 allows its NZ atom to form a water bridge with the carbonyl O atom of Ala57 of a (001)-translated molecule. The NZ atom of Lys115 forms two hydrogen bonds, one with a water molecule ($d = 2.7$ Å) and another with the carbonyl O atom of Asp58 ($d = 3.3$ Å) of a (1–10)-translated molecule. Such intermolecular interactions are not seen in wild-type PCaM.

The PCaM has 18 sequence changes from MCaM and 17 changes from DCaM (Fig. 1). Most of the sequence changes are conservative and the differences are at positions, 17, 86, 99 and 147. Therefore, it is not surprising that the rPCaM is very similar in structure to those of other calmodulin structures (Babu *et al.*, 1985, 1988; Krestinger, Rudnick & Weissman, 1986; Taylor *et al.*, 1991). Superposition of our structure (residues 5–147) with MCaM yields an r.m.s. deviation of 0.44 Å for 143 equivalent C^{α} atoms. It is seen that the C-terminal domain (r.m.s. = 0.45 Å) and the central helix (r.m.s. 0.45 Å) have a slightly higher r.m.s. deviation than the N-terminal domain (r.m.s. = 0.43 Å) (Fig. 10). The reason for this is probably to the fact that 17 of the 18 sequence changes between the two calmodulin molecules are in the central helix region and the C-terminal domain. In the structure of rPCaM, the OE1 atom of Glu83 forms a hydrogen bond with the NE2 atom of Gln79 ($d = 3.2$ Å) and the side chain of Glu139 forms a salt bridge with the side chain of Arg143 ($d = 2.7$ Å). In

Table 12. *R.m.s. deviation and backbone torsion angles for the four regions where the residues have more than 1.3 Å deviation for equivalent C^{α} atoms between rPCaM and rDCaM*

Residue number	Residues in PCaM/DCaM	R.m.s. deviation (Å)	Torsion angles (°) of rPCaM φ	Torsion angles (°) of rPCaM ψ	Torsion angles (°) of rDCaM φ	Torsion angles (°) of rDCaM ψ
N-terminal and *A*-helical regions						
1	A/A	13.38		17		150
2	E/D	8.02	−176	117	−55	151
3	Q/Q	1.40	−168	−176	−129	−40
4	L/L	1.59	−147	133	−13	154
5	L/T	1.43	−82	162	−78	−170
6	E/E	1.57	−53	−35	−93	−17
7	E/E	1.21	−73	−36	−76	−35
8	Q/Q	1.34	−67	−43	−69	−49
9	I/I	1.32	58	−47	70	−20
10	A/A	1.31	−60	−42	−87	−26
B/*C* linker region						
44	T/T	1.08	−83	163	−120	155
45	E/E	1.55	−53	−45	−40	−54
46	A/A	1.70	−63	−38	−53	−44
47	E/E	1.29	−66	−42	−66	−48
F helix and *F*/*G* linker regions						
106	R/R	0.92	−72	−38	−64	−52
107	H/H	1.12	−63	−42	−50	−56
108	V/V	0.94	−67	−35	−56	−67
109	M/M	1.01	−67	−31	−38	−32
110	T/T	1.17	−69	−41	−104	−8
111	N/N	2.15	−66	−21	−82	−21
112	L/L	2.50	−87	4	−99	−63
113	G/G	1.31	95	15	180	−9
114	E/E	1.14	−120	104	−116	153
H-helix and C-terminal regions						
145	M/M	1.77	−71	−37	−69	78
146	V/T	2.75	−75	−13	−171	−64
147	S/S	2.01	−53	−30	−58	−49
148	K/K	4.62	−17		−140	

MCaM, Glu82 forms a salt bridge with Arg86 (d = 2.2 Å). The latter salt bridge is not present in rPCaM because residue 86 is Ile86. All these differences occur in the helical regions which may account for the small conformational differences between the two calmodulin molecules. The crystal structures of the two recombinant calmodulins, rPCaM and rDCaM, show rather high deviation (r.m.s. = 1.67 Å for all C^{α} atoms) compared with MCaM (Figs. 10 and 11). Significantly large deviations (> 1.3 Å) are found for residues 1–10, 44–47, 106–114 and 144–148 (Table 12). Most of these residues have different backbone conformations.

The central helical region shows significant differences among the rPCaM, MCaM and rDCaM structures. There are two kinks in the MCaM at Lys75 and Ile85 and one kink in rDCaM at Asp80. These kinks increase the distance between the carbonyl and amide groups at these positions. The distances between the carbonyl O atom ($C{=}O_i$) and the amide N (N_{i+4}) atom are beyond the optimal value for the formation of the α-helix hydrogen

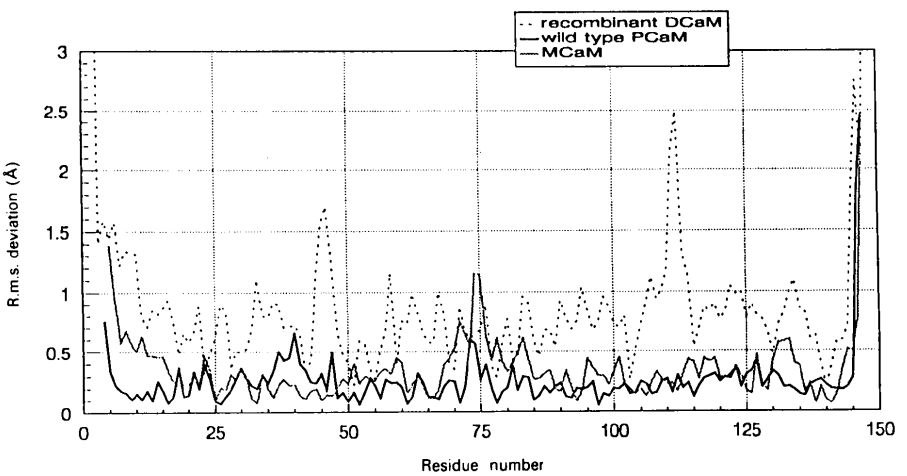

Fig. 10. A plot of the deviations for equivalent C^{α} atoms between rPCaM and the other calmodulin structures.

bond. Initially, it was thought that the increase in the separation of $C{=}O_i$ and N_{i+4} groups was as a result of the presence of a water bridge (Sundaralingam & Sekharudu, 1989). But on examination of the structures, no water molecules were found. In contrast the present structure and our previous wild-type PCaM structure showed normal hydrogen-bonding distances between $C{=}O_i$ and N_{i+4} atoms and normal φ, ψ dihedral angles typical of an α-helix with little or no bending (Table 6).

Structure and dynamics – functional implications

The conformational dynamics of the dumbbell molecule may involve kinking or bending of the central helix by disrupting the direct helix hydrogen bonds to form a random structure for the *D/E* linker. The presence of a large number of water molecules bound to the central helix in rPCaM suggests that the right-angle bend in the *D/E* helices in the calmodulin–peptide complex may be preceded by water molecules inserting into the *D/E* linker helix hydrogen bonds prior to the disruption of the helix (Sundaralingam & Sekharudu, 1989). Thus, the helix-to-random-coil transition in the linker region of the long helix is presumably what happens during the folding of calmodulin to form the calmodulin–MLCK peptide complex.

Various natural mutants of PCaM affect the Na^+ and K^+ ion channels in *Paramecium*. Mutations that reduce the calmodulin-dependent Na^+ inward current are confined to the N-terminal domain; those that reduce the calmodulin-dependent K^+ outward current are in the C-terminal domain revealing that the two domains have different specific interactions with different ion-channel peptides (Kink *et al.*, 1990). The precisely determined calmodulin structure will form the basis of our further studies on calmodulin mutants.

Note: After this paper was completed, a high-resolution (1.7 Å) structure of rDCaM (Chattopadhyada, Meador, Means & Quiocho, 1992) was published where the four N-terminal residues were now not found to be ordered (absent) and the central helix was more regular and intact, as in our rPCaM.

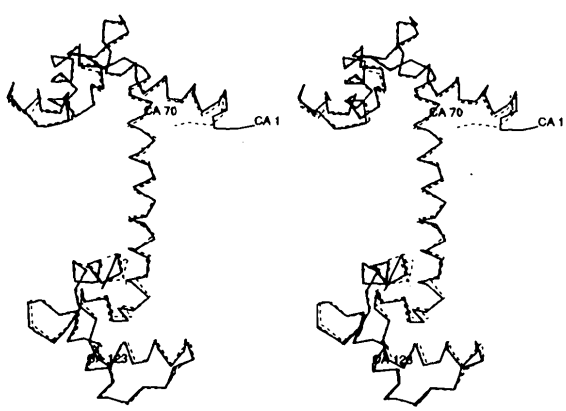

Fig. 11. Stereoview of the superposition of the C^α atoms between rPCaM and rDCaM; the solid line indicates the rPCaM and the dotted line indicates the rDCaM. View is selected in such a way that the different conformations of the four N-terminal residues of both structures are seen clearly.

We thank Drs S. T. Rao and C. Sekharudu for helpful discussions. The protein preparation studies were supported by NIH grants GM-22714 and GM-36386 to CK. The X-ray crystallographic studies were supported by an endowment from the Regents of the Ohio State University to MS. We also thank the Ohio State Supercomputer Center for a grant of computer time on the Cray Y-MP/864.

References

BABU, Y. S., BUGG, C. E. & COOK, W. J. (1988). *J. Mol. Biol.* **204**, 191–204.

BABU, Y. S., SACK, J. S., GREENHOUGH, T. J., BUGG, C. E., MEANS, A. R. & COOK, W. J. (1985). *Nature (London)*, **315**, 37–40.

BERNSTEIN, F. C., KOETZLE, T. F., WILLIAMS, G. J. B., MEYER, E. F. JR, BRICE, M. D., RODGERS, J. R., KENNARD, O., SHIMANOUCHI, T. & TASUMI, M. (1977). *J. Mol. Biol.* **112**, 535–542.

BLUNDELL, T., BARLOW, D., BORKAKOTI, N. & THORNTON, J. (1983). *Nature (London)*, **306**, 281–283.

BRÜNGER, A. T. (1990). *X-PLOR Manual.* Version 2.1. Yale Univ., New Haven, CT, USA.

BURGER, D., COX, J. A., COMTE, M. & STEIN, E. A. (1984). *Biochemistry*, **23**, 1966–1971.

CHATTOPADHYADA, R., MEADOR, W. E., MEANS, A. R. & QUIOCHO, F. A. (1992). *J. Mol. Biol.* **228**, 1177–1192.

COX, J. A., CORUTE, M., MAMAR-BACHI, A., MILOS, M. & SCHAER, J. J. (1988). *Cation Binding to Calmodulin and Relation to Function*, edited by C. GERDAY, L. BOLIS & R. R. GILES, pp. 141–162. New York: Springer Verlag.

EINSPAHR, H. & BUGG, C. E. (1984). *Crystal Structure Studies of Calcium Complexes and Implications for Biological Systems. Metal Ions in Biological Systems*, Vol. 17, edited by H. SIGEL, pp. 51–97. New York: Marcel Deckker.

GREGORI, L., MARRIOTT, D., PUTKEY, J. A., MEANS, A. R. & CHAU, V. (1987). *J. Biol. Chem.* **262**, 2562–2567.

HERZBERG, O. & JAMES, M. N. G. (1988). *J. Mol. Biol.* **203**, 761–779.

HOWARD, A. J., NIELSEN, C. & XUONG, N. H. (1985). *Methods Enzymol.* **114**, 452–472.

IKURA, M., CLORE, G. M., GRONENBORN, A. M., ZHU, G., KLEE, C. B. & BAX, A. (1992). *Science*, **256**, 632–638.

JONES, T. A. (1985). *Methods Enzymol.* **115**, 157–171.

LUKAS, T. J., BURGESS, W. H., PENDERGAST, F. G., LAU, W. & WATTERSON, D. M. (1986). *Biochemistry*, **25**, 1458–1464.

KEMP, B. E., PEARSON, R. B., GUERRIERO, V., BAGCHI, I. C. & MEANS, A. R. (1987). *J. Biol. Chem.* **262**, 2542–2548.

KINK, J. A., MALEY, M. E., LING, K.-Y., KANABROCHI, J. & KUNG, C. (1991). *J. Protozool.* **38**, 441–447.

KINK, J. A., MALEY, M. E., PRESTON, R. R., LING, K.-Y., WALLEN-FRIEDMAN, M. A., SAIMI, Y. & KUNG, C. (1990). *Cell*, **62**, 165–174.

KLEE, C. B. & VANAMAN, T. C. (1982). *Adv. Protein Chem.* **35**, 213–321.

KRETSINGER, R. H. & NOCKOLDS, C. E. (1973). *J. Biol. Chem.* **248**, 3313–3326.

KRETSINGER, R. H., RUDNICK, S. E. & WEISSMAN, L. J. (1986). *J. Inorg. Biochem.* **28**, 289–302.

LUZZATI, P. V. (1952). *Acta Cryst.* **5**, 802–810.

MEADOR, W. E., MEANS, A. R. & QUIOCHO, F. A. (1992). *Science*, **257**, 1251–1255.

MEANS, A. R., TASH, J. S. & CHAFOULEAS, J. G. (1982). *Physiol. Rev.* **62**, 1–39.

NEWTON, D. L., OLDEWURTEL, M. D., KRINKS, M. H., SHILOACH, J. & KLEE, C. B. (1984). *J. Biol. Chem.* **259**, 4419–4426.

PERSECHINI, A. & KRETSINGER, R. H. (1988). *J. Biol. Chem.* **263**, 12175–12178.

RAO, S. T., WU, S., SATUSHUR, K., LING, K.-Y., KUNG, C. & SUNDARALINGAM, M. (1993). *Protein Sci.* **2**, 436–447.

SATYSHUR, K. A., PYZALSKA, D., RAO, S. T., GREASER, M. & SUNDARALINGAM, M. (1994). *Acta Cryst.* D**50**, 40–49.

SATYSHUR, K. A., RAO, S. T., PYZALSKA, D., DRENDEL, W., GREASER, M. & SUNDARALINGAM, M. (1988). *J. Biol. Chem.* **263**, 16028–16047.

SEKHARUDU, Y. C. & SUNDARALINGAM, M. (1988). *Protein Eng.* **2**, 139–146.

SEKHARUDU, Y. C. & SUNDARALINGAM, M. (1993*a*). *Protein Sci.* **2**, 620–625.

SEKHARUDU, Y. C. & SUNDARALINGAM, M. (1993*b*). *Hydration of Protein Secondary Structures. The Role in Protein Folding*, Vol. 17, edited by E. WESTOF, pp. 149–162. Cambridge Univ. Press.

STRYNADKA, N. C. J. & JAMES, M. N. G. (1989). *Annu. Rev. Biochem.* **58**, 951–998.

STRYNADKA, N. C. J. & JAMES, M. N. G. (1990). *Proteins Struct. Funct. Genet.* **7**, 234–248.

SUNDARALINGAM, M. & SEKHARUDU, Y. C. (1989). *Science*, **244**, 1333–1337.

TANAKA, T. & HIDAKA, H. (1980). *J. Biol. Chem.* **255**, 11078–11080.

TAYLOR, D. A., SACK, J. S., MAUNE, J. F., BECKINGHAM, K. & QUIOCHO, F. A. (1991). *J. Biol. Chem.* **266**, 21375–21380.

WNUK, W. (1988). *Calcium and Calcium Binding Proteins*, edited by C. H. GERDAY, L. BOLIS & R. GILLES, pp. 44–68. New York: Springer Verlag.